Title

A Hydrologic Modeling Assessment of Future Water Scarcity in the Baitarani River Basin

ISBN

9783031765315

Authors

Swain, Sushree Swagatika

Mishra, Ashok

Chatterjee, Chandranath

et al.

Publication Date

2025

DOI

10.1007/978-3-031-76532-2_20

Chapter 20
A Hydrologic Modeling Assessment of Future Water Scarcity in the Baitarani River Basin

Sushree Swagatika Swain, Ashok Mishra, Chandranath Chatterjee, and Morgan C Levy

Abstract Water scarcity, defined as an adverse imbalance between freshwater availability and water demand, is a critical concern in the 21st century, and is exacerbated by climate change and increased uncertainties in hydrological cycles. Rising water demands driven by rapid population growth, urbanization, and industrialization further intensify water scarcity, posing significant threats to sustainable development. Addressing water scarcity is particularly challenging in regions with limited data availability, and data constraints can necessitate the use of a water balance approach to quantify water scarcity. Evaluating the hydrological balance of river basins in historical and projected future time periods requires the use of hydrologic and climatic models, wherein the selection of an appropriate model and modelling approach depends on research objectives, data accessibility, site-specific challenges, costs, and model accuracy. In response to these conditions, this study explores hydrological model-based estimates of water scarcity risk in the absence of sector-specific water demand data. Specifically, this study evaluates streamflow, 'blue' and 'green' water balance components derived from streamflow, and a risk-based measure of water scarcity calculated from those water balance components in the Baitarani river basin (13,000 km^2), a basin influenced by climate and land use change. This analysis relies on historical observed climate and hydrologic data (1974–2018) from the Indian Meteorological Department (IMD) and Central Water Commission (CWC), modelled future climate (2020–2064) from the Coupled Model Intercomparison Project 6 (CMIP6), and the Soil Water Assessment Tool (SWAT) hydrologic model.

S. S. Swain (✉)
Scripps Institution of Oceanography, University of California San Diego, San Diego, CA, USA
e-mail: ssswain@ucsd.edu

A. Mishra · C. Chatterjee
Agricultural and Food Engineering Department, Indian Institute of Technology Kharagpur, Kharagpur, India
e-mail: amishra@agfe.iitkgp.ac.in; cchatiit@gmail.com

M. C. Levy
Scripps Institution of Oceanography and School of Global Policy and Strategy, University of California San Diego, San Diego, CA, USA
e-mail: mclevy@ucsd.edu

A. Nanda et al. (eds.), *Navigating the Nexus*, Water Science and Technology Library 102, https://doi.org/10.1007/978-3-031-76532-2_20

This study finds that Baitarani basin water scarcity has decreased in recent decades (1994–2018) relative to earlier decades (1974–1993), and that water scarcity risk will also decrease in the future (2020–2064). Nevertheless, findings remain uncertain due to limited model structural representation of hydrologic processes that may change alongside land use and climate change drivers. Even so, this study offers valuable insights for parsimoniously evaluating basin-scale water availability and scarcity, aiding in the development of adaptive strategies for sustainable water management in data-scarce river basins.

Keywords Water scarcity · Water availability · Climate change · Blue water flow · Green water flow · Green water storage · CMIP6

20.1 Introduction

The World Economic Forum (WEF) has identified water scarcity as one of the top three global systemic risks of utmost concern, based on a comprehensive global survey encompassing stakeholders from business, academia, civil society, governments, and international organizations (World Economic Forum 2014). Water scarcity, defined as a deficit in the supply of freshwater relative to water demand, is a critical concern in water-stressed regions, as water availability and access have extensive impacts on both human societies and ecosystems (Pedro-Monzonís et al. 2015; Veldkamp et al. 2017; Sun and Zhou 2020). Concerns about water scarcity are amplified in regions with rapid economic development, particularly in emerging economies (Abedzadeh et al. 2020). Increasing water demand due to population growth, industrialization, and agricultural expansion, coupled with climate change and anthropogenic activities, intensify water scarcity challenges (Wada et al. 2011; UN World Water Development Report 2021). Urbanization along with climate change can accelerate water scarcity at local to regional scales (Wu et al. 2023), where water scarcity affects food security, access to safe drinking water, and public health (Taylor 2009). Furthermore, many international and interstate river basins are expected to face water scarcity in coming decades (Beck and Bernauer 2011; Gain and Giupponi 2015), posing additional challenges to transboundary water management (Kryston et al. 2022).

The quantification of "blue" surface—and groundwater and "green" rainwater as sources of available water is important for addressing the impacts of water scarcity (Hoekstra 2016), but water scarcity is determined by both physical and social factors, and their interactions. Thus, understanding and addressing water scarcity also requires assessments that extend beyond simple water supply and demand analyses to include socio-economic factors such as governance systems and policies (Falkenmark et al. 2007). Ideally, water scarcity research considers the complex interactions of climate change, variations in human activities, and their impacts on hydrologic responses. "Socio-hydrologic" research (Sivapalan et al. 2012) that bridges coupled physical and social dynamics that govern water scarcity, however,

faces challenges such as data scarcity and anthropogenic feedback (Müller and Levy, 2019). For instance, assessing water scarcity risk under the non-availability of basin-scale sectoral water demands and socio-economic factors limits capacity to execute socio-hydrologic research in data-scarce river basins (Swain et al. 2020). Thus, water scarcity risk research that relies on modelling of physical climate and readily observable proxies for various forms of human activity, such as Land Use/ Land Cover (LULC), are a practical and parsimonious approach to analysing water scarcity given inherent complexity.

Model-based analyses of water scarcity frequently acknowledge the multifaceted influences of climate change and/or LULC dynamics on hydrological systems and provide straightforward management-relevant findings (Ayeni et al. 2015; Chanapathi & Thatikonda, 2020; Dosdogru et al. 2020; Omer et al. 2020; Mechal et al. 2022; Dolgorsuren et al. 2024; Li et al. 2024). Modelling can be used quantify the dependence of hydrological processes on precipitation patterns, temperature regimes, and LULC variations (Chen et al. 2020; Jose et al. 2021; Kayitesi et al. 2022; Gupta et al. 2024), and simulations of change in hydrology enable stakeholders to anticipate shifts in water availability and plan adaptation measures accordingly. A widely used hydrological model for the estimation of hydrological response to climate variability and change, as well as LULC, is the Soil and Water Assessment Tool (SWAT), which is a which is a quasi-distributed, physically-based hydrologic model (Srinivisan et al. 1998; Tan et al. 2020). SWAT model analyses have been used to assess quality and quantity of surface and ground water, the impact of LULC and climate change on hydrologic responses, prevention and control of soil erosion, control of point and non-point source pollution, ecosystem assessment and regional river basin management (Tan et al. 2020; Aloui et al. 2023; Dubey et al. 2023; Uniyal et al. 2023; Zhao et al. 2024). Given that uncertainties in climate projections and LULC scenarios challenge accurate prediction within any hydrologic model (Wagener et al. 2010), including but not limited to SWAT, the integration of risk-based approaches into water scarcity analysis with hydrological model output is necessary (Veldkamp et al. 2017).

While a focus on LULC within hydrologic modelling can simplify representations of human activity, and model input and output uncertainty can be acknowledged to a certain extent using a risk framing, fundamental modelling design challenges remain. Specifically, land use and climate change dynamics are embedded in hydrologic records that represent reference conditions in model experiments. Identifying points of change in hydrologic records over time remains an essential step in many hydrologic modelling efforts, as the selection of "baseline" and "assessment" periods underpin quantifications of change. Thus, use of 'change point', 'breakpoint', or 'turning point' approaches, which indicate points in time at which time series data split into subsets with distinct statistical properties, can be used to establish comparative time periods (Friedman et al. 2016).

Change points within datasets indicate non-stationarities, a concept widely employed for identifying and evaluating the timing and magnitudes of hydro-climatic change at multiple scales (Xie et al. 2019; Zhou et al. 2019), and can indicate abrupt shifts in variables like precipitation, streamflow, reservoir storage, urbanization or

agricultural practices (Ryberg et al. 2020). As a result, change points in long-term hydro-climatic data have been used to evaluate water scarcity across comparison time periods (Rafiei-Sardooi et al. 2022). There are several change point detection methods such as the Bayesian Change-Point (BCP) approach (Wang et al. 2018), parametric change-point analysis (Killick and Eckley, 2014), non-parametric change-point analysis (Haynes et al. 2021), and the trend-based approach (Pettitt test) (Pettitt, 1979). However, selecting suitable change point detection methods and then identifying change points within long-term hydro-climatic data are both processes that are subject to inherent uncertainties and limitations related to data quality and availability (He et al. 2022). At a minimum, approaches that are suitable for hydrologic applications avoid invalid statistical assumptions (i.e., normality and independence) and have the capacity to detect multiple change points (Ryberg et al. 2020). Ideally, approaches can identify sequential trends with varying lengths and slopes (Şen, 2019).

It remains that the accuracy of water scarcity risk estimation and projection at the basin scale alone depends on myriad model structural and forcing data factors: representations of time-varying climate, LULC, hydrologic processes, and human intervention. Nevertheless, applied management-relevant research must proceed with estimation in the absence of one or more of these factors. Thus, the question of what parsimonious hydrologic modelling approaches yield in river basins, despite limitations, is valid insofar as the model results are used to understand the future 'possibility space' (Baldassarre et al. 2019). Thus, based on the above critical appraisal, the present study aims to analyse water availability and water scarcity conditions in long-term historical as well as future scenarios in the Baitarani river basin of Eastern India, a basin that has undergone substantial land use change and faces significant projections of hydroclimatic change (Srivastava and Maity, 2023).

This study does so using a SWAT model simulation approach, and using data inputs that include 45 years of observed historical climate and hydrologic data (1974–2018), historical land cover maps (1985, 2005), and 40 years of projected future climate (2020-2059) from two Shared Socioeconomic Pathway (SSP) scenarios from the Coupled Model Intercomparison Project 6 (CMIP6). The flowchart of the overall methodology is shown in Figure 20.1. This study narrates the development of an applied hydrologic model-driven analysis of climate and land use change in a historical reference period, and climate change (with static land use) in a future period, as well as comparisons across time periods and future scenarios. Results from this study illustrate what is, and is not, typically possible in the case of an applied water scarcity risk analysis in a data-scarce basin. Furthermore, model simulation findings and their interpretation highlight the potentially important but often omitted role of model structural representations within management-focused studies of water resources change.

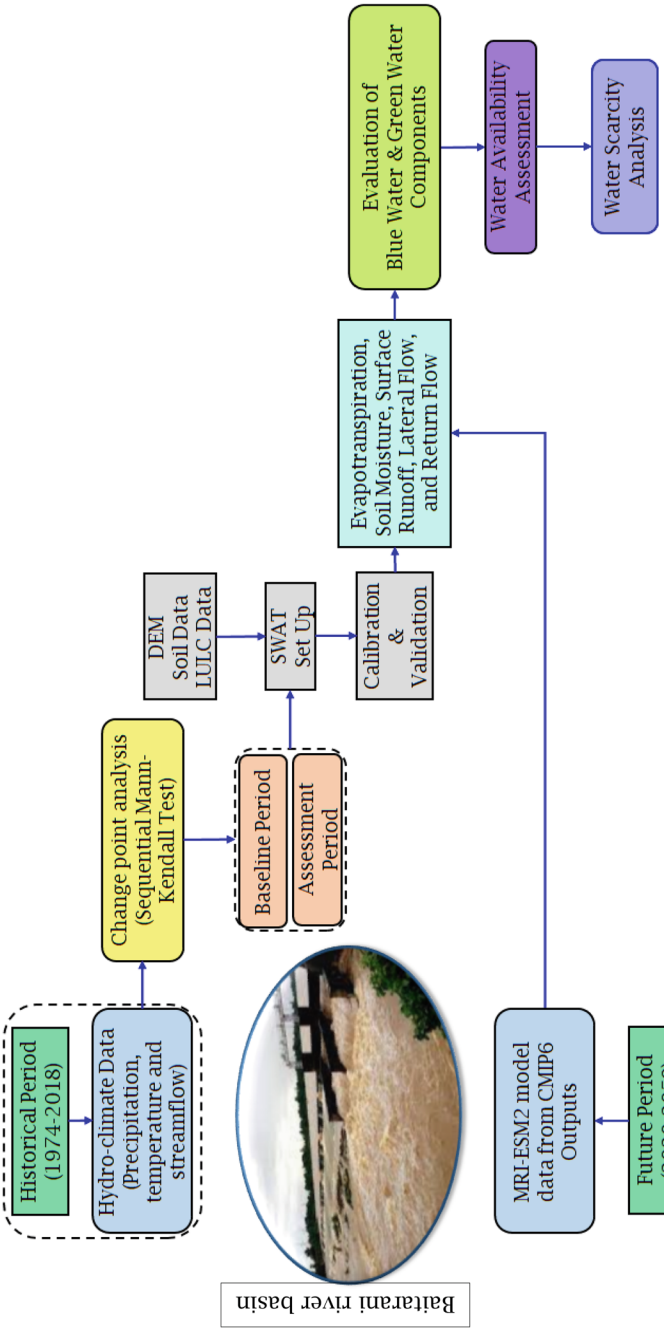

Fig. 20.1 Flowchart for the overall methodology framework of this study.

20.2 Background of the Study Area

The Baitarani river basin is an interstate basin in Eastern India that spans approximately 12,094 km^2, and the river has a travelling length of 360 km before draining into the Bay of Bengal. It extends from 20°30′ N to 22°20′ N in latitude and 85°05′ E to 87°05′ E in longitude (Figure 20.2). Covering primarily the regions of Odisha and a smaller portion of Jharkhand, the Baitarani river basin is a major regional catchment known for its agriculture, fisheries and industrial sectors, and the basin includes a wide variety of land-use types such as agricultural land, water bodies, fallow and wasteland, forested areas and developed/urban land (Visakh et al. 2019). In this basin, the Anandapur streamflow gauging station is located upstream of the Salandi Dam (Figure 20.2), constructed between 1974 and 1983, enabling assessment of variations in unimpaired hydrologic responses with climate change and LULC (Swain et al. 2020). The Salandi Dam is the major water management structure in the Baitarani river basin, storing floodwaters during the monsoon season and supplying water to agriculture and industry during periods of high demand.

The Baitarani river basin falls within a subtropical monsoon climate zone, and the monsoon months (June–September) are the primary source of precipitation, contributing approximately 80% of annual rainfall (Swain et al. 2020). Earlier studies have identified the study area as flood-prone (Rai et al. 2018; Dahm et al. 2019) and simultaneously drought-prone according to projections of increased drought occurrence and magnitudes under future climate change (Ojha et al. 2013; Suman and Maity, 2021). Studying water availability and water scarcity in the context of these divergent and changing extremes poses an illustrative modelling challenge.

20.3 Data Sources

The necessary input data for SWAT consists of the Digital Elevation Model (DEM), LULC maps, soil and meteorological data, and streamflow time series data for model calibration and validation. The details of the data are given as follows:

20.4 Spatial Data Sources

The DEM is sourced from the Shuttle Radar Topography Mission (SRTM), offering a spatial resolution of 30 m × 30 m (Farr et al. 2007; NASA JPL, 2013). Statics derived from soil property maps rely on the Food and Agriculture Organization (FAO) Harmonized World Soil Database (HWSD) v1.2 (Fisher et al. 2008; FAO, 2012), with a spatial scale of 1 km by 1 km. The Decadal LULC Classifications across India dataset provides satellite-derived LULC classifications at a decadal temporal resolution and with a spatial resolution of 100 m by 100 m (Roy et al. 2016). To

Fig. 20.2 Location and—map of the Baitarani river basin.

analyse the impact of LULC changes during the reference period, representative land cover maps for the years 1985 and 2005 are employed.

20.5 Historical Hydro-Climatic Data Sources

The time period represented by historical data is 1974–2018. The primary observed meteorological data (precipitation, min and max temperature) are obtained on a daily scale from the India Meteorological Department (IMD), Pune (Rajeevan et al. 2006; Pai et al. 2015). The spatial resolution of obtained precipitation data is 0.25°. The obtained 1° gridded temperature data is rescaled to 0.25° resolution through a widely used bilinear interpolation approach (Almazroui et al. 2017, 2020) to maintain spatial consistency with the obtained precipitation data (Swain et al. 2021; Dey et al. 2022). The daily observed streamflow data is collected from the Anandpur (21° 13' 46" N, 86° 7' 30" E) gauging station made available by the Central Water Commission (CWC), Bhubaneswar, and has been extensively used in various applied hydrologic studies (Rai et al. 2018; Visakh et al. 2019; Swain et al. 2023, 2024).

20.6 Future Climatic Data Sources

Global Climate Models (GCMs) are widely employed to simulate and project climate change on both a global and regional scale and are regarded as essential for water resources management research (Fan et al. 2020; Xu et al. 2021). By using standardized simulations within a variety of GCMs, the Coupled Model Intercomparison Project (CMIP) enables quantification of uncertainties in future climate projections across models. GCMs from the sixth phase of CMIP (CMIP6) have delivered substantial enhancements over their previous model generation (CMIP5) in horizontal resolution, physical parameterizations (e.g., cloud representation), the addition of other Earth system processes (like nutrient limitations to the terrestrial carbon cycle) and added components (e.g., ice sheets) (Eyring et al 2016, 2019). A set of socioeconomic and technological development scenarios, collectively known as the Shared Socioeconomic Pathways (SSPs), are developed in CMIP6. SSPs differ from prior CMIP5 Representative Concertation Pathway (RCP) scenarios by describing challenges to adaptation and mitigation, in addition to emissions as presented in the Special Report on Emissions Scenarios (SRES) of the Intergovernmental Panel on Climate Change (IPCC) (O'Neill et al. 2017). The CMIP6 SSP scenarios combine two dimensions, the RCP representation of the severity of climate change (represented by emissions levels), and the SSP narrative characterization of five directions of global societal development (Kriegler et al. 2014). The five SSPs portray alternative pathways of socioeconomic development, such as sustainable development (SSP1), middle-of-the-road development (SSP2), regional rivalry (SSP3), inequality (SSP4) and fossil-fuelled development (SSP5) (Meinshausen et al. 2019).

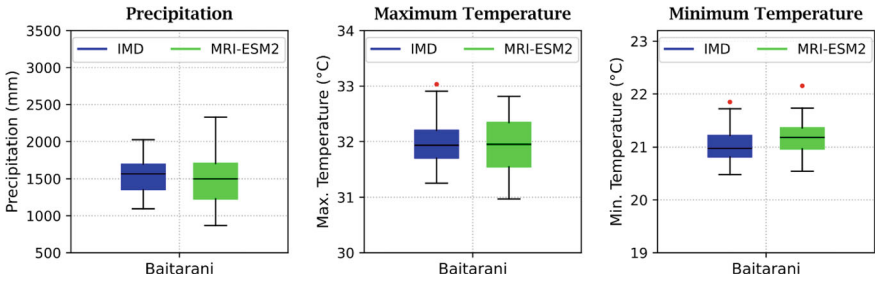

Fig. 20.3 Box and whisker representation of observed IMD and modelled MRI-ESM2 climate variables.

In this study, SSP245 and SSP585 scenarios from CMIP6 are selected to represent future water availability and scarcity under medium and high emission scenarios, respectively. Bias-corrected CMIP6 precipitation, maximum temperature and minimum temperature at a 0.25° × 0.25° spatial resolution and daily temporal resolution come from the Bias Corrected Climate Projections from CMIP6 Models for South Asia dataset (Mishra et al. 2020). These bias-corrected future datasets are widely used for hydro-climatic analysis in the South Asia region (Pandey et al. 2022; Das et al. 2023; Swain et al. 2023). Out of the 13 available GCMs, the MRI-ESM2 model is selected for its superior regional performance, relative to other GCMs, over the modelled historical period (Mahato et al. 2022). Figure 20.3 depicts the annual precipitation and temperature (maximum and minimum) from the observed IMD and modelled MRI-ESM2 spanning the years 1979–2014. There is good agreement between the IMD data and the bias-corrected MRI-ESM2 model data within the study area. Bias-corrected MRI-ESM2 data from the period of 2020–2059 is then used to represent the future period.

20.7 Methodology

20.7.1 Change Point Detection Analysis

This study uses the Sequential Mann–Kendall test for the identification of multiple change points in the historical hydrologic data, and is used to partition the historical period into baseline and assessment periods. The Sequential version of the Mann–Kendall test was initially formulated by Sneyers, 1990, and was subsequently modified and applied in hydrological studies (Douglas et al. 2000; Yang and Tian, 2009; Zhao et al. 2015; Dey and Mishra; 2017; Nourani et al. 2018). Using comparisons between progressive (forward) and retrograde (backward) sequences of ranked time series data, this method detects change points as the onset of trends in those data. The rank of mean annual streamflow magnitudes X_j (where $j = 1, 2, \ldots, n$) are compared to the rank of X_k (where $k = 1, 2, \ldots, j\text{-}1$). The number of events in which the rank

of X_k exceeds the rank of X_j is denoted by n_j. The test statistic (T_j) is then calculated based on these counts and given by:

$$T_j = \sum_1^j n_j \ (j = 2, 3, ..., n) \tag{20.1}$$

The test statistics are assumed to be normally distributed. The mean and variance of the test statistics are estimated as:

$$E(T) = \frac{n(n-1)}{4} \tag{20.2}$$

$$\mathrm{Var}(T_j) = \frac{\left[j(j-1)(2j+5)\right]}{72} \tag{20.3}$$

The sequential values of the statistic $U(T_j)$ are calculated as:

$$U(T_j) = \frac{T_j - E(T_j)}{\sqrt{\mathrm{Var}(T_j)}} \tag{20.4}$$

which is called the progressive series. Similarly, the retrograde series $U'(T_j)$ is generated in the same way, but with a reversed original time series. The null hypothesis is accepted if $|U(T_j)|$ is less than or equal to $U(T_j)_{1\text{-}\alpha/2}$; where α is the significance level at which the two-sided trend test is performed. The critical value ($U(T_j)_{1\text{-}\alpha/2}$) represents the threshold of the standard normal distribution with a probability greater than $\alpha/2$. A positive $U(T_j)$ indicates a positive trend, while the negative $U(T_j)$ signifies a negative trend, with $U'(T_j)$ reflecting the same pattern as $U(T_j)$. The Sequential Mann–Kendall test in this study is performed at a 5% significance level. The change points in the hydrologic variable (streamflow) are observed at the point where the progressive and retrograde series intersect with each other, and the null hypothesis of there being no trend in the data is rejected for the entire sample if any of the sequential statistics $U(T_j)$ exceed the confidence interval (i.e., +/− 1.96). Here, the intersection point with the greatest sequential statistic value is used to indicate the break point in the long-term streamflow data series. Thus, the study period (i.e. reference period) is partitioned into a baseline period and an assessment period using the year corresponding to the greatest positive value of $U(T_j)$.

20.8 Linear Trend Analysis

The linear trend test is a statistical method frequently used in the hydrology domain to identify and quantify trends in hydro-climatic variables over time, such as precipitation, streamflow, and temperature, providing understanding of long-term changes in water resources and climate patterns (Zhou et al. 2023; Wu et al. 2024). In this study, the linear trend test is performed to evaluate change in annual summaries (e.g., total

precipitation, mean streamflow and temperature) of hydro-climatic variables during the reference, baseline and assessment periods, with a significance level set at 5%.

20.9 SWAT Model-Based Scenario Definition

The basin-scale modelling of the study area is done using the SWAT2012 interface (Arnold et al. 2012) with an ArcGIS 10.3-ArcView extension (Wang et al. 2020). SWAT enables representation of various physical hydrological processes, including streamflow, groundwater flow, evapotranspiration, lateral flow and percolation. Streamflow is generated using the SCS curve number method and routed through the Muskingum channel routing method. Evapotranspiration in this study is quantified by the Penman-Monteith method. Subsurface flow components, including groundwater flow, lateral flow and percolation, are assessed through the mass balance of the subsurface system. The conceptualization of hydrological processes in SWAT is presented through the water balance equation, which is formulated as:

$$\mathrm{SW}_t = \mathrm{SW}_o + \sum_{i=1}^{t} (P_i - Q_i - ET_i - G_i - R_i) \tag{20.5}$$

where SW_t is the residual water content in the soil, SW_o is the initial soil water content on ith day, t is time in days, P_i is the precipitation on ith day, Q_i is the surface runoff on ith day, ET_i is the evapotranspiration (ET) on ith day, G_i is the water flowing to the subsurface zone from the soil profile on ith day, and R_i is the return flow on ith day.

SWAT model setups (Table 20.1) are designed around the baseline and assessment time periods that were determined through the change point analysis, and these periods represent alternative climatic and LULC conditions. A warm-up period of 2 years is incorporated for both baseline and assessment periods. The Baitarani river basin is calibrated at the Anandpur gauging station using the SUFI-2 algorithm within the SWAT-CUP interface at a monthly scale (Abbaspour, 2014). Sensitivity analysis of model parameters is conducted using the LH-OAT sampling approach (Van Griensven and Meixner, 2007). The performance of the calibrated and validated models is assessed using three performance indicators: the coefficient of determination (R^2), the Nash-Sutcliffe Efficiency (NSE), and the Percent Bias (PBIAS).

$$R^2 = \left[\sum_{i=1}^{n} \left(Q_i^o - \overline{Q^o}\right)\left(Q_i^m - \overline{Q^m}\right)\right]^2 \Bigg/ \sum_{i=1}^{n} \left(Q_i^o - \overline{Q^o}\right)^2 \sum_{i=1}^{n} \left(Q_i^m - \overline{Q^m}\right)^2 \tag{20.6}$$

$$\mathrm{NSE} = 1 - \left|\sum_{i=1}^{n} \left(Q_i^o - Q_i^m\right)^2 \Bigg/ \sum_{i=1}^{n} \left(Q_i^o - \overline{Q^o}\right)^2\right| \tag{20.7}$$

Table 20.1 Details of the historical time periods for SWAT modelling.

Time frame	LULC	Climate
Baseline period	1985	1974–1993
Assessment period	2005	1994–2018

$$\text{PBIAS} = \left(\sum_{i=1}^{n} \left(Q_i^m - Q_i^o \right) \times 100 \right) \Big/ \sum_{i=1}^{n} Q_i^o \tag{20.8}$$

where $\overline{Q^o}$ is the observed mean streamflow, Q_i^o is the ith observed streamflow, Q_i^m is the ith model-simulated streamflow, $\overline{Q^m}$ is the model-simulated mean streamflow and n is the total number of the data points. The calibrated and validated SWAT model is then used to simulate future hydrology using CMIP6 climate for the period of 2020–2059. Due to the assessed compatibility between historical CMIP6 climate and observed historical climate (Figure 20.2), a SWAT run of historical period CMIP6 climate was deemed unnecessary.

20.10 Blue/ Green Water Availability Analysis

Water availability is assessed using blue and green water components constructed from SWAT outputs. Blue Water Flow (BWF) is calculated by aggregating surface water and groundwater components. Hence, surface runoff/ streamflow, lateral flow and return flow are combined to form the BWF components at a basin scale. The concept of naturally infiltrated water forms the basis of the green water component in a basin, which is estimated using two terms. Firstly, Green Water Storage (GWS) represents the available moisture in the soil. Secondly, the Green Water Flows (GWF) denote the actual evapotranspiration, which is the loss of water from the soil by release to the atmosphere through a combination of transpiration from vegetative and evaporation from water bodies and soil profiles. Therefore, in the present study, BWF and GWS are considered indicators of water availability in that they are used to quantify water scarcity. Further, Water Availability (WA) is defined as the summation of BWF and GWS components (i.e., total water available is surface water and groundwater). It is important to note that the derived estimates for the water balance components are analysed directly from model-simulated outputs due to the lack of available observational data.

20.11 Framework Water Scarcity-Risk Analysis

Water scarcity is usually assessed by comparing sectoral water demands with the available water resources at the basin scale. However, the details of sectoral water demand data are limited in many river basins, including the Baitarani basin. Thus, water scarcity risk assessment is performed in this study based on relative changes in streamflow (ΔQ) and Water Availability (ΔWA) for baseline and assessment periods. It is assumed that there is a state of equilibrium between water demands and water availability for this analysis, which means that the amount of water needed by different sectors (agriculture, industry, households, etc.) is assumed to be balanced by the water available from BWS and GWS. The relative changes in streamflow and water availability are calculated as follows:

$$\Delta Q = \frac{Q_a - Q_b}{Q_b} \tag{20.9}$$

$$\Delta \mathrm{WA} = \frac{\mathrm{WA}_a - \mathrm{WA}_b}{\mathrm{WA}_b} \tag{20.10}$$

The relative change in streamflow (ΔQ) is calculated as the ratio of the difference between the average streamflow for the assessment period (Q_a) and the baseline period (Q_b) to the average streamflow for the baseline period (Q_b). Similarly, the relative change in water availability (ΔWA) is determined as the ratio of the difference between the average water availability for the assessment period (WA_a) and the baseline period (WA_b) to the average water availability for the baseline period (WA_b).

Based on the parameter values outlined above, four distinct risk zones are identified, following the criteria proposed in earlier studies (Garrote et al. 2018; Swain et al. 2020). The criteria for potential water scarcity risk assessment zoning are as follows:

$$\begin{aligned}
\text{Zone1 } (\mathrm{Z}_1) &= (\Delta Q > 0,\ \Delta \mathrm{WA} > 0) = \text{Less risk} \\
\text{Zone2 } (\mathrm{Z}_2) &= (\Delta Q < 0,\ \Delta \mathrm{WA} > 0) = \text{Moderate risk} \\
\text{Zone3 } (\mathrm{Z}_3) &= (\Delta Q > 0,\ \Delta \mathrm{WA} < 0) = \text{High risk} \\
\text{Zone4 } (\mathrm{Z}_4) &= (\Delta Q < 0,\ \Delta \mathrm{WA} < 0) = \text{Extreme risk}
\end{aligned}$$

Zone 1 represents low water scarcity risk, wherein water demands exceed water availability, and is represented by positive changes in both streamflow and water availability. Zone 2 signifies a moderate risk of water scarcity due to decreased streamflow (only). Zone 3 indicates a high water scarcity risk due to reduced water availability (only). In zone 4, where both streamflow and water availability decrease, the basin faces an extreme risk of water scarcity and is likely to experience hydrological drought conditions in the region (Goyal et al. 2017). The assessment of water scarcity includes a change point analysis of streamflow, a linear trend analysis of hydro-climate variables, and an evaluation of their impact on water availability.

This impact analysis relies on the calibrated and validated SWAT outputs over the reference (baseline and assessment) period. Water scarcity in the reference period is assessed by comparing water availability and streamflow in the baseline and assessment periods. Then, water scarcity in the future period is assessed by comparing the reference period with SSP245 and SSP 585 hydro-climate variables, respectively.

20.12 Results and Discussions

20.12.1 Change Point Detection Analysis

The Sequential Mann–Kendall test statistic calculated on streamflow data from the Anandapur station in the Baitarani basin identified a total of 11 change points (Table 20.2, Figure 20.4).

Table 20.2 Sequential Mann–Kendal test statistics in the reference period.

Year	Sequential statistic
1978	0.92
1983	2.01
1985	1.63
1989	2.21
1991	1.93
1993	2.32
2002	1.69
2009	1.09
2011	1.11
2012	1.19

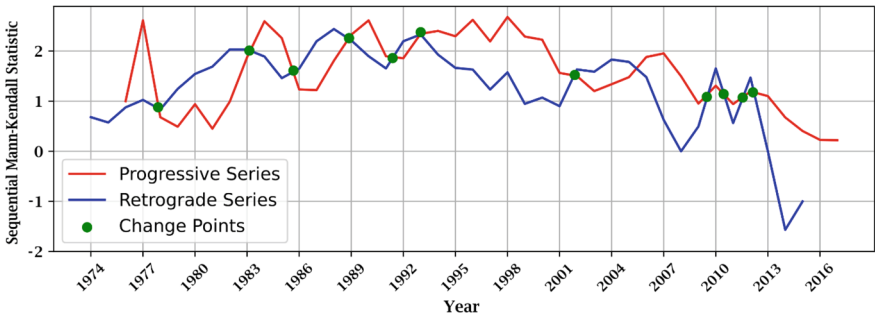

Fig. 20.4 Change points identified by the Sequential Mann–Kendall test of streamflow in the reference period.

Between 2010 and 2013, there are three change points with almost identical sequential statistic values (1.1–1.2). Similarly, in the years 1983 and 1993, sequential statistic values greater than 2 are observed, with the year 1993 exhibiting the greatest value of 2.32. Based on these results, the full reference period of 1974–2018 is divided into two sub-periods: the period before the change point with the greatest corresponding sequential statistic value (1974–1993) is considered to be the baseline period, while the period after (1994–2018) is termed the assessment period.

20.13 Hydro-Climatic and LULC Change Statistics in Reference Period

Comparisons of the trends in the hydro-climatic variables across different periods are illustrated in Figure 20.5. In the reference period from 1974 to 2018, precipitation shows a positive trend ($\Delta = 3.65$ mm/year), though there is no statistical significance (p-value $= 0.2$). Similarly, streamflow has a negligible downward trend ($\Delta = -0.17$ m^3/s/year) during the reference period, which is not statistically significant (p-value $= 0.805$). However, temperature displays a consistent and statistically significant upward trend ($\Delta = 0.01$ °C/year, p-value $= 0.020$) over this period. In the baseline period from 1974 to 1993, precipitation exhibits a significant upward trend ($\Delta =$ 13.37 mm/year^2) without any statistical significance (p-value $= 0.102$). Streamflow also demonstrates a significant upward trend ($\Delta = 3.06$ m^3/s/year) during the baseline period, but not significant (p-value $= 0.123$). Similarly, temperature shows no statistically significant trend during this period. Finally, in the assessment period from 1994 to 2018, precipitation displays a slight downward trend ($\Delta = -1.44$ mm/year), though not statistically significant (p-value $= 0.845$). Streamflow, however, reveals a significant downward trend ($\Delta = -3.03$ m^3/s/year), approaching statistical significance (p-value $= 0.088$). Temperature continues its upward trend ($\Delta = 0.02$ °C/year) during the assessment period, and is statistically significant (p-value $= 0.016$). Overall, while precipitation and streamflow exhibit varying trends with statistical insignificance across different periods, temperature consistently displays a significant upward trend, which is especially noticeable in the reference and assessment periods.

The LULC maps of 1985 and 2005 were selected to represent the baseline period and assessment periods, respectively. Summaries of basin LULC classes by time period are shown in Figure 20.6. Between 1985 and 2005, agricultural land increased slightly from 56.22% to 56.89%, indicating continued agricultural expansion. Conversely, deciduous forests experienced a decline from 28.06% to 24.15%, suggesting deforestation or land conversion activities. Fallow land remained relatively stable at 1.35% throughout both periods. Shrubland and mixed forest areas showed modest increases, indicating possible reforestation or natural growth processes. The proportion of water bodies also saw a slight rise from 1.58% to 1.82%, reflecting potential changes in hydrological features. Urban land exhibited a

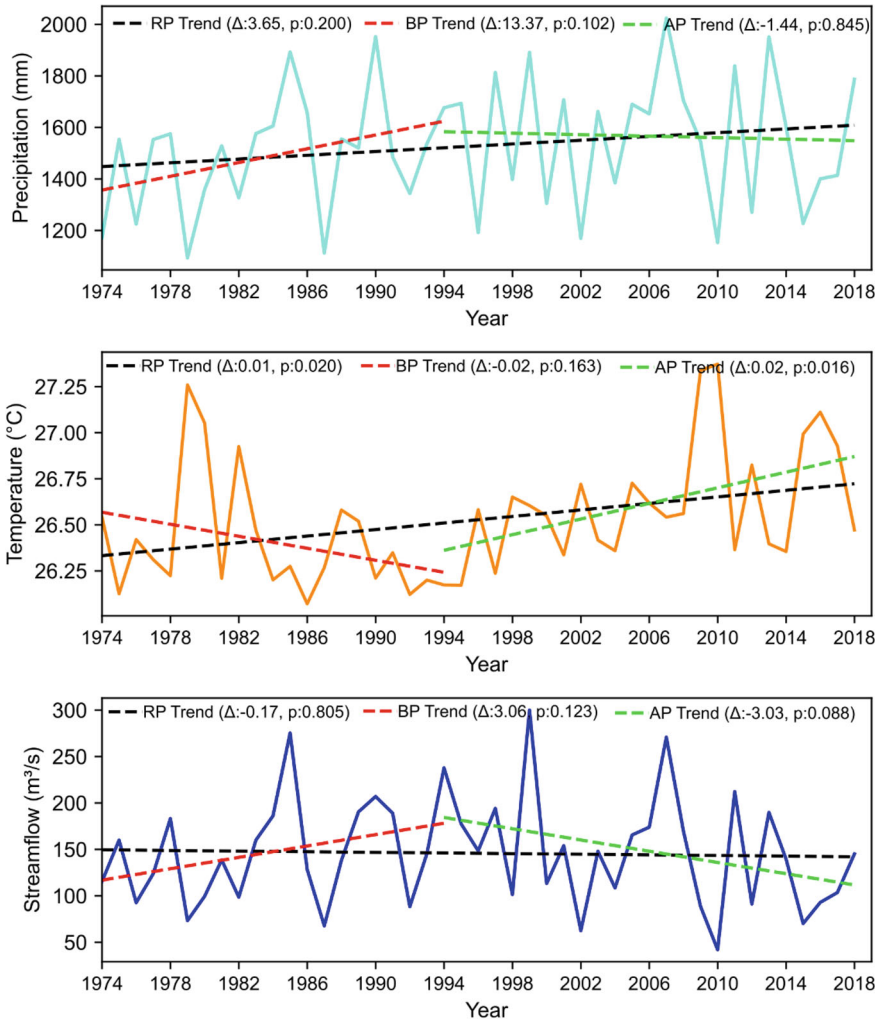

Fig. 20.5 Linear trend variation of annual hydro-climatic variables for different periods.

minor increase from 1.04% to 1.23%, indicating limited urbanization or infrastructure development. These changes highlight shifts in land use patterns over the two decades, with implications for ecosystem health, biodiversity, and water resource management within the study area.

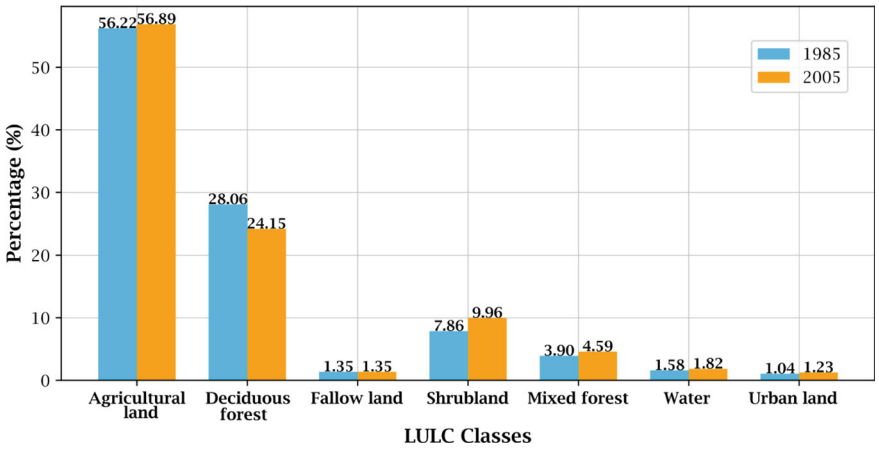

Fig. 20.6 LULC percentages within the Baitarani river basin during baseline (1985) and assessment (2005) years of the reference period.

20.14 SWAT Model Scenario Execution

The two SWAT model setups of baseline and assessment periods, as outlined in Table 20.1, are calibrated and validated using 10 parameters that the model is particularly sensitive to according to earlier literatures (Paul et al. 2019; Visakh et al. 2019; Swain et al. 2020, 2021, 2023). The selected sensitive parameters with suitable ranges and fitted values are detailed in Table 20.3. Sensitive parameters and their ranges are determined through a comprehensive model calibration of the study area. The calibrated peak flow is fine-tuned by adjusting sensitive parameters such as the curve number (CN2.mgt) and available water capacity of the soil layer (SOL_AWC.Sol), drawing from insights gained in earlier studies (Abbaspour et al. 2015). Parameters such as the groundwater delay time (GW_DELAY.gw), threshold depth of water in the shallow aquifer required for return flow to occur (GWQMN.gw), and the groundwater revap coefficient (GW_REVAP.gw) are employed to modify the baseflow of the study area. Changes in LULC are anticipated to influence the variability of sensitive model parameters (Das et al. 2018; Swain et al. 2021), as well as the streamflow response of the basin. The calibration and validation periods are selected based on a ratio of approximately 60:40, respectively. For the baseline period (1974–1993), the model is calibrated from 1974 to 1985 and validated from 1986 to 1993. Similarly, for the assessment period (1994–2018), the model is again calibrated from 1994 to 2008 and validated for the years from 2009 to 2018.

Figure 20.7 illustrates the comparisons of monthly streamflow time series between model simulations and observed streamflow at the Anandapur station. The model results demonstrate an acceptable level of agreement between observed and model-simulated streamflow. The statistical performance indices used to evaluate model performance, including NSE values exceeding 0.5, R2 values above 0.6, and PBIAS

Table 20.3 Best-fit sensitive parameters of model calibration in the study area.

Parameters	Description	Range	Fitted value	
			Baseline period	Assessment period
CN2	Initial SCS runoff number for moisture condition II	(70,90)	80.53	77.30
GW_DELAY	Groundwater delay time (days)	(30,450)	53.94	37.98
ALPHA_BF	Baseflow alpha factor (1/days)	(0,1)	0.40	0.72
GWQMN	Threshold depth of water in the shallow aquifer required for return flow to occur (mm H_2O)	(0,5000)	2755	2695
CH_K2	Effective hydraulic conductivity in main channel alluvium (mm/h)	(0,200)	11.49	38.70
CH_N2	Manning's n value for the main channel	(0,0.3)	0.07	0.10
ALPHA_BNK	Base flow alpha factor for bank storage (days)	(0,1)	0.47	0.91
SOL_AWC	Available water capacity of the first soil layer (mm H_2O/mm soil)	(0,1)	0.20	0.17
REVAPMN	Threshold of evaporation in the shallow aquifer (mm)	(0,500)	273	19.5
GW_REVAP	Groundwater 'revap' coefficient	(0.02,0.2)	0.11	0.12

values falling within ±25, suggest reliability of the model (Moriasi et al. 2007). The NSE, R^2 and PBIAS values for the calibration period and validation period of the respective model scenarios are outlined in Figure 20.7. During the calibration of the baseline period, the model exhibits an NSE of 0.81 and R^2 of 0.88, indicating a good fit between observed and simulated streamflow values. The PBIAS value of 12.27 suggests a slight overestimation of the observed values. During validation, the model performance improves slightly, with NSE and R^2 values of 0.84 and 0.90, respectively, and a higher PBIAS value of 16.76, indicating a larger overestimation in the validation period. In the calibration period of the assessment period, the model exhibits a slight decrease in performance compared to the baseline period, showing NSE and R^2 values of 0.79 and 0.82, respectively and a negative PBIAS value of − 13.14, indicating an underestimation of observed values. However, in the assessment period validation, the model performance improves, with NSE and R^2 values of 0.83 and 0.88, respectively and a further reduction in PBIAS to − 19.56, indicating a larger underestimation. Overall, the model performance indicators suggest satisfactory performance across different time scales, with some variation in performance

metrics between calibration and validation periods and between baseline and assessment periods. Subsequently, the model is simulated for different future SSPs based on the calibrated model parameters of the assessment period.

20.14.1 Assessment of Water Availability

Figure 20.8 presents summaries of estimated blue and green water components (BWF, GWF and GWS), alongside precipitation, across the different time periods and SSPs. In the reference period (baseline and assessment periods combined), the average precipitation is recorded as 247.02 mm, with corresponding values for BWF, GWF, and GWS of 201.055, 21.3 and 24.76 mm, respectively. In the baseline period, there is slightly less precipitation of 245.38 mm, while other components also exhibit minor differences. In the assessment period, precipitation increases very slightly to 248.29 mm, leading to a corresponding slight rise in BWF, GWF and GWS. SSP585 exhibits significantly higher precipitation and BWF, while maintaining the same GWF and only slightly higher GWS compared to the reference period. Both SSP scenarios show similar GWS levels, which are only marginally higher than those in the reference period. This indicates that evaporative and subsurface processes as represented in the SWAT model are unchanged from the reference period, and thus GWS changes only to the extent that increases in BWF propagate through the representation of those processes.

Future SSP simulations only include future climate change in this study, and calibrated SWAT representation of dynamical land surface and subsurface hydrologic processes are unchanged from the reference period. In reality, future LULC dynamics can significantly impact water availability by altering surface runoff, groundwater recharge and evapotranspiration processes, as documented in earlier studies conducted in various regions around the world (Levy et al. 2018; Tankpa et al. 2021; Sinha et al. 2023; Ebodé et al. 2024). For example, the expansion of urban areas or conversion of natural habitats to agricultural land can lead to increased surface runoff and reduced infiltration rates, potentially exacerbating flood risks and reducing groundwater recharge. Conversely, afforestation efforts or restoration of degraded landscapes may enhance water retention and infiltration capacities, mitigating runoff and improving groundwater replenishment (Brown et al. 2005; Zhang et al. 2017). From a modelling perspective, such changes would alter calibration of SWAT model parameters, resulting in change additional to that which is generated by climate alone. It remains that this study's representation of the two baseline and assessment period LULC types, along with their corresponding observed climate, yielded only marginal change in water availability components over the reference period.

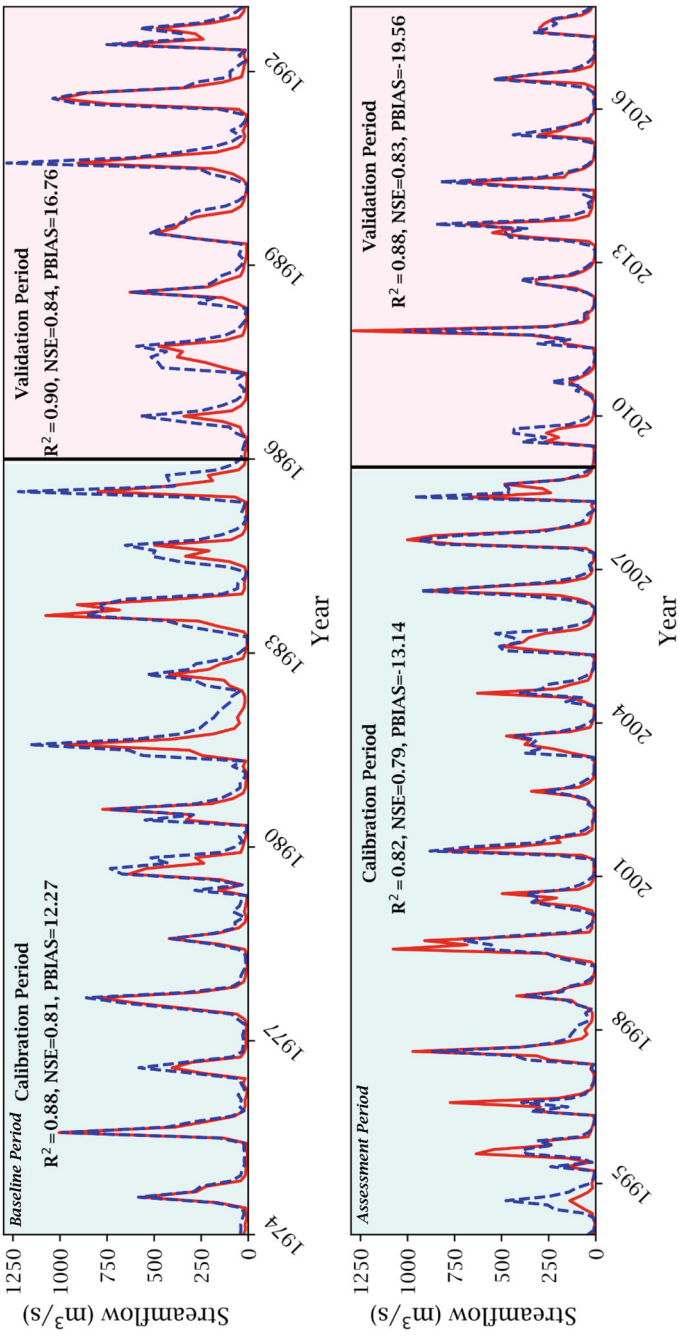

Fig. 20.7 SWAT model performances in the baseline and assessment periods

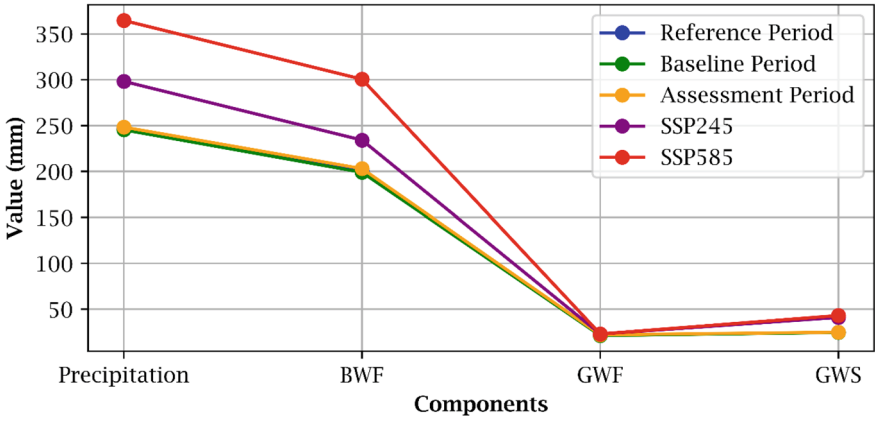

Fig. 20.8 Water availability assessment for different periods.

20.15 Water Scarcity Risk Analysis

The calculation of water scarcity based on streamflow and water availability is assessed at a basin scale and presented in Figure 20.9. The figure represents the changes in water availability (WA) and streamflow (Q) between different periods (reference, baseline, and assessment periods) and scenarios (SSP245 and SSP585), indicating potential shifts in water scarcity risk zoning. In the comparison between the baseline period and the assessment period, there is a marginal increase in water availability (0.02) but a sizable increase in streamflow (0.08). Overall, this generates reduced risk of water scarcity primarily due to enhanced runoff. Comparing the reference period with the SSP245 and SSP585 scenarios (RP-SSP245 and RP-SSP585, respectively), both scenarios show increases in water availability and streamflow. However, the SSP585 scenario exhibits a larger increase in water availability (0.52) compared to SSP245 (0.22); both exhibit relative changes of 0.04 for streamflow.

According to the water scarcity-risk criteria (as defined in subsection 4.4), positive relative changes in both WA and Q, which represents a situation wherein both terms are greater relative to a comparison period, suggests lower water scarcity risk. A positive change in water availability implies an increase in the overall water supply, while a positive change in streamflow indicates higher runoff and potentially improved replenishment of water resources. Thus, in this model simulation experiment, and when manipulating primarily climate variability and change via the use of alternative time periods and CMIP6 SSPs, water scarcity is expected to decrease in the Baitarani river basin in the future.

This conclusion faces several limitations. While the assumption of equilibrium between water demands and water availability simplifies the analysis, the dynamic and variable nature of water supply and demand is influenced by numerous factors such as seasonal variations, population growth, economic development and climate change, which limits understanding of water scarcity risks. This study also uses a

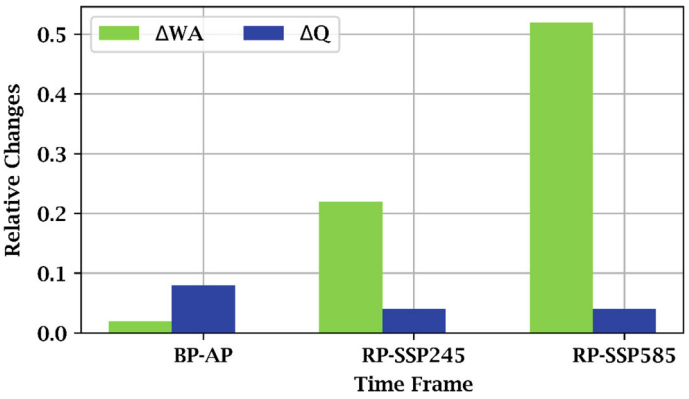

Fig. 20.9 Relative changes in streamflow and water availability for different comparison periods.

hydrologic model whose process representations (e.g., parameterizations) are representative of a static historical period. In contrast to that representation, a study by Garrote et al. (2018) suggested that basin-scale water availability is determined by a combination of streamflow and variable hydrological responses represented by water storage components. Such variable hydrologic responses are not incorporated in this study. One way to do so would be to integrate future LULC scenarios and corresponding parameterizations, along with future climate, into the analysis to assess the combined effects of climate and land use change on hydrologic responses and water scarcity more comprehensively (Leta et al. 2021; Acharya et al. 2023). This would provide valuable insights not only into potential trade-offs and relations between different land management strategies and climate adaptation measures, but also understanding about the extent to which model structural representations are important for understanding future risk of water scarcity.

20.16 Conclusions

This study evaluates modelled water scarcity in an observed historical reference period (1974–2018) and under simulated future climate (2020–2059), alongside representative land use/land cover (LULC) conditions. Using a Sequential Mann–Kendall change point analysis, this study identifies the year (1993) of the most significant change in historical Baitarani river basin streamflow. The subsequent use of this change point analysis to partition the historical reference data into baseline (1974–1993) and assessment periods (1994–2018) represents the use of a data-driven approach to guide otherwise subjective modelling decisions under uncertainty. This study then finds that the SWAT model performs satisfactorily in capturing the dynamic changes in LULC throughout both the baseline and assessment periods. Additionally, modelled blue and green water components yield fluctuations in water

availability across the baseline and assessment periods, and in future SSP scenarios. In particular, SSP585 hydrology had notably higher quantities of blue water relative to other time periods, indicating the potentially strong influence of extreme precipitation on water resources in the study region. Building from the analysis of blue and green water components, the analysis of water scarcity indicates that the relative changes in water availability and streamflow are positive for the assessment period, as well as for the SSP245 and SSP585 scenarios, suggesting that the Baitarani basin will face reduced water scarcity risk in the future.

The findings of this study offer valuable insights for making informed decisions and managing water resources effectively in data-limited river basins, especially given the evolving dynamics of climate and changes in land use and land cover. Nevertheless, limitations remain. Here, consideration of future LULC scenarios alongside future climate would enhance the robustness of the model structural representation of hydrologic change, and thereby offer water resource management and planning efforts greater certainty in projected future streamflow and water availability.

Acknowledgement The authors are thankful to the India Meteorological Department (IMD), Pune and the Central Water Commission (CWC), Bhubaneswar for providing the hydro-meteorological datasets required for conducting this study.

References

Abbaspour KC, Rouholahnejad E, Vaghefi S, Srinivasan R, Yang H, Kløve B (2015) A continental-scale hydrology and water quality model for Europe: calibration and uncertainty of a high-resolution large-scale SWAT model. J Hydrol 524:733–752

Abbaspour KC (2014) SWAT-CUP 2012: SWAT calibration and uncertainty programs-a user manual: swiss federal institute of aquatic science and technology

Abedzadeh S, Roozbahani A, Heidari A (2020) Risk assessment of water resources development plans using fuzzy fault tree analysis. Water Resour Manage 34(8):2549–2569

Acharya S, Hori T, Karki S (2023) Assessing the spatio-temporal impact of landuse landcover change on water yield dynamics of rapidly urbanizing Kathmandu valley watershed of Nepal. J Hydrol Reg Stud 50:101562

Almazroui M, Nazrul Islam M, Saeed S, Alkhalaf AK, Dambul R (2017) Assessment of uncertainties in projected temperature and precipitation over the Arabian Peninsula using three categories of Cmip5 multimodel ensembles. Earth Syst Environ 1:1–20

Almazroui M, Saeed S, Saeed F, Islam MN, Ismail M (2020) Projections of precipitation and temperature over the South Asian countries in CMIP6. Earth Syst Environ 4:297–320

Aloui S, Mazzoni A, Elomri A, Aouissi J, Boufekane A, Zghibi A (2023) A review of soil and water assessment tool (SWAT) studies of mediterranean catchments: applications, feasibility, and future directions. J Environ Manage 326:116799

Arnold JG, Moriasi DN, Gassman PW, Abbaspour KC, White MJ, Srinivasan R, Santhi C, Harmel RD, Van Griensven A, VanLiew MW, Kannan N, Jha MK (2012) SWAT: model use, calibration, and validation. Trans ASABE 55(4):1491–1508

Ayeni AO, Kapangaziwiri E, Soneye ASO, Engelbrecht FA (2015) Assessing the impact of global changes on the surface water resources of southwestern Nigeria. Hydrol Sci J 60(11):1956–1971

Beck L, Bernauer T (2011) How will combined changes in water demand and climate affect water availability in the Zambezi river basin? Glob Environ Chang 21(3):1061–1072

Brown AE, Zhang L, McMahon TA, Western AW, Vertessy RA (2005) A review of paired catchment studies for determining changes in water yield resulting from alterations in vegetation. J Hydrol 310(1–4):28–61

Chanapathi T, Thatikonda S (2020) Investigating the impact of climate and land-use land cover changes on hydrological predictions over the Krishna river basin under present and future scenarios. Sci Total Environ 721:137736

Chen Q, Chen H, Zhang J, Hou Y, Shen M, Chen J, Xu C (2020) Impacts of climate change and LULC change on runoff in the Jinsha River Basin. J Geog Sci 30(1):85–102

Dahm RJ, Sperna Weiland FC, Singh UK, Lal M, Marchand M, Singh SK, Singh MP (2019) Assessment of future rainfall for the Brahmani–Baitarani river basin–practical implications of limited data availability. J Water Climate Change 10(4):782–798

Das P, Behera MD, Patidar N, Sahoo B, Tripathi P, Behera PR, Krishnamurthy YVN (2018) Impact of LULC change on the runoff, base flow and evapotranspiration dynamics in eastern Indian river basins during 1985–2005 using variable infiltration capacity approach. J Earth Syst Sci 127(2):1–19

Das J, Das S, Umamahesh NV (2023) Population exposure to drought severities under shared socioeconomic pathways scenarios in India. Sci Total Environ, 161566

Dey P, Mishra A (2017) Separating the impacts of climate change and human activities on streamflow: a review of methodologies and critical assumptions. J Hydrol 548:278–290

Dey A, Remesan R (2022) Multimodel quantification of green and blue water components and its error propagations through parameter transferability approach across input choices. J Hydrol 607:127579

Di Baldassarre G, Sivapalan M, Rusca M, Cudennec C, Garcia M, Kreibich H, Blöschl G (2019) Sociohydrology: scientific challenges in addressing the sustainable development goals. Water Resour Res 55(8):6327–6355

Dolgorsuren SE, Ishgaldan B, Myagmartseren P, Kumar P, Meraj G, Singh SK, Kanga S, Almazroui M (2024) Hydrological responses to climate change and land-use dynamics in central Asia's semi-arid regions: an SWAT model analysis of the Tuul River Basin. Earth Syst Environ

Dosdogru F, Kalin L, Wang R, Yen H (2020) Potential impacts of land use/cover and climate changes on ecologically relevant flows. J Hydrol 584:124654

Douglas EM, Vogel RM, Kroll CN (2000) Trends in floods and low flows in the United States: impact of spatial correlation. J Hydrol 240(1–2):90–105

Dubey SK, Kim J, Her Y, Sharma D, Jeong H (2023) Hydroclimatic impact assessment using the SWAT model in India—State of the art review. Sustainability 15(22):15779

Ebodé VB, Onana JYN, Boyomo TMS (2024) Water resources availability in the Mefou basin, Cameroon: under current and future climate, and land use and land cover. Sustain Water Resour Manag 10(2):78

Eyring V, Bony S, Meehl GA, Senior CA, Stevens B, Stouffer RJ, Taylor KE (2016) Overview of the Coupled Model Intercomparison Project Phase 6 (CMIP6) experimental design and organization. Geosci Model Dev 9(5):1937–1958

Eyring V, Cox PM, Flato GM, Gleckler PJ, Abramowitz G, Caldwell P, Williamson MS (2019) Taking climate model evaluation to the next level. Nat Clim Chang 9(2):102–110

Falkenmark M, Berntell A, Jägerskog A, Lundqvist J, Matz M, Tropp H (2007) On the verge of a new water scarcity: a call for good governance and human ingenuity. SIWI Policy Brief. SIWI

FAO (2012) Harmonized world soil database (version 1.2). Food and Agriculture Organization, Rome, Italy, and IIASA, Laxenburg, Austria

Fan X, Duan Q, Shen C, Wu Y, Xing C (2020) Global surface air temperatures in CMIP6: historical performance and future changes. Environ Res Lett 15(10):104056

Farr TG et al (2007) The shuttle radar topography mission. AGU J

Fisher MJ et al (2008) Harmonized world soil database v1.2

Friedman D, Schechter J, Baker B, Mueller C, Villarini G, White KD (2016) US army corps of engineers nonstationarity detection tool user guide. US Army Corps of Engineers, Washington, DC

Gain AK, Giupponi C (2015) A dynamic assessment of water scarcity risk in the Lower Brahmaputra River Basin: an integrated approach. Ecol Ind 48:120–131
Garrote L, Iglesias A, Granados A (2018) Country-level assessment of future risk of water scarcity in Europe. Proceed Int Assoc Hydrol Sci 379:455–462
Goyal MK, Gupta V, Eslamian S (2017) Hydrological drought: water surface and duration curve indices. In: Handbook of drought and water scarcity. CRC Press. pp 45-71
Gupta V, Syed B, Pathania A, Raaj S, Nanda A, Awasthi S, Shukla DP (2024) Hydrometeorological analysis of July-2023 floods in Himachal Pradesh, India. Natural Hazards, 1-26
Haynes K, Killick R, Fearnhead P, Eckley I (2021) Changepoint. np. Methods for nonparametric changepoint detection. R package version 1.0. 3
He Q, Wang M, Liu K, Li K, Jiang Z (2022) GPRChinaTemp1km: a high-resolution monthly air temperature data set for China (1951–2020) based on machine learning. Earth Syst Sci Data 14(7):3273–3292
Hoekstra AY (2016) A critique on the water-scarcity weighted water footprint in LCA. Ecol Ind 66:564–573
Jose DM, Makhdumi W, Dwarakish GS (2021) Hydrological Modelling to Study the Impacts of Climate and LULC Change at Basin Scale: A Review. In: Jha R, Singh VP, Singh V, Roy LB, Thendiyath R (eds) Water resources management and reservoir operation: hydraulics, water resources and coastal engineering. Springer International Publishing, pp 13–26
Kayitesi NM, Guzha AC, Mariethoz G (2022) Impacts of land use land cover change and climate change on river hydro-morphology—a review of research studies in tropical regions. J Hydrol 615:128702
Killick R, Eckley IA (2014) Changepoint: an R package for changepoint analysis. J Stat Softw 58:1–19
Kriegler E, Edmonds J, Hallegatte S, Ebi KL, Kram T, Riahi K, Van Vuuren DP (2014) A new scenario framework for climate change research: the concept of shared climate policy assumptions. Clim Change 122:401–414
Kryston A, Müller MF, Penny G, Bolster D, Tank JL, Mondal MS (2022) Addressing climate uncertainty and incomplete information in transboundary river treaties: a scenario-neutral dimensionality reduction approach. J Hydrol 612:128004
Leta MK, Demissie TA, Tränckner J (2021) Hydrological responses of watershed to historical and future land use land cover change dynamics of Nashe watershed Ethiopia. Water 13(17):2372
Levy MC, Lopes AV, Cohn A, Larsen LG, Thompson SE (2018) Land use change increases streamflow across the arc of deforestation in Brazil. Geophys Res Lett 45(8):3520–3530
Li Y, Huang Y, Li Y, Zhang H, Fan J, Deng Q, Wang X (2024) Spatiotemporal heterogeneity in meteorological and hydrological drought patterns and propagations influenced by climatic variability, LULC change, and human regulations. Sci Rep 14(1):5965
Mahato PK, Singh D, Bharati B, Gagnon AS, Singh BB, Brema J (2022) Assessing the impacts of human interventions and climate change on fluvial flooding using CMIP6 data and GIS-based hydrologic and hydraulic models. Geocarto Int 37(26):11483–11508
Mechal A, Takele T, Meten M, Deyassa G, Degu Y (2022) A modeling approach for evaluating the impacts of Land Use/Land Cover change for Ziway Lake watershed hydrology in the Ethiopian Rift. Model Earth Syst Environ 8(4):4793–4813
Meinshausen M, Nicholls Z, Lewis J, Gidden MJ, Vogel E, Freund M, Wang HJ (2019) The SSP greenhouse gas concentrations and their extensions to 2500. Geosci Model Dev Discuss 2019:1–77
Mishra V, Bhatia U, Tiwari AD (2020) Bias corrected climate projections from CMIP6 models for South Asia. Zenodo
Moriasi DN, Arnold JG, Van Liew MW, Bingner RL, Harmel RD, Veith TL (2007) Model evaluation guidelines for systematic quantification of accuracy in watershed simulations. Trans ASABE 50(3):885–900
Müller MF, Levy MC (2019) Complementary vantage points: Integrating hydrology and economics for sociohydrologic knowledge generation. Water Resour Res 55(4):2549–2571

NASA JPL (2013) Shuttle radar topography mission (SRTM)
Nourani V, Danandeh Mehr A, Azad N (2018) Trend analysis of hydroclimatological variables in Urmia lake basin using hybrid wavelet Mann–Kendall and Şen tests. Environ Earth Sci 77(5):1–18
O'Neill BC, Kriegler E, Ebi KL, Kemp-Benedict E, Riahi K, Rothman DS, Solecki W (2017) The roads ahead: Narratives for shared socioeconomic pathways describing world futures in the 21st century. Glob Environ Chang 42:169–180
Ojha R, Nagesh Kumar D, Sharma A, Mehrotra R (2013) Assessing severe drought and wet events over India in a future climate using a nested bias-correction approach. J Hydrol Eng 18(7):760–772
Omer A, Elagib NA, Zhuguo M, Saleem F, Mohammed A (2020) Water scarcity in the Yellow River Basin under future climate change and human activities. Sci Total Environ 749:141446. https://doi.org/10.1016/j.scitotenv.2020.141446
Pai DS, Sridhar L, Badwaik MR, Rajeevan M (2015) Analysis of the daily rainfall events over India using a new long period (1901–2010) high resolution (0.25× 0.25) gridded rainfall data set. Climate Dyn 45(3):755–776
Pandey D, Tiwari AD, Mishra V (2022) On the occurrence of the observed worst flood in Mahanadi River basin under the warming climate. Weather Climate Extremes 38:100520
Paul PK, Gaur S, Kumari B, Panigrahy N, Mishra A, Singh R (2019) Diagnosing credibility of a large-scale conceptual hydrological model in simulating streamflow. J Hydrol Eng 24(4):04019004
Pedro-Monzonís M, Solera A, Ferrer J, Estrela T, Paredes-Arquiola J (2015) A review of water scarcity and drought indexes in water resources planning and management. J Hydrol 527:482–493. https://doi.org/10.1016/j.jhydrol.2015.05.003
Pettitt AN (1979) A non-parametric approach to the change-point problem. J Roy Stat Soc: Ser C (Appl Stat) 28(2):126–135
Rafiei-Sardooi E, Azareh A, Joorabian Shooshtari S, Parteli EJR (2022) Long-term assessment of land-use and climate change on water scarcity in an arid basin in Iran. Ecol Model 467:109934. https://doi.org/10.1016/j.ecolmodel.2022.109934
Rai PK, Dhanya CT, Chahar BR (2018) Coupling of 1D models (SWAT and SWMM) with 2D model (iRIC) for mapping inundation in Brahmani and Baitarani river delta. Nat Hazards 92:1821–1840
Rajeevan M, Bhate J, Kale JD, Lal B (2006) High resolution daily gridded rainfall data for the Indian region: analysis of break and active monsoon spells. Curr Sci, 296-306
Roy PS, Meiyappan P, Joshi PK, Kale MP, Srivastav VK, Srivasatava SK, Krishnamurthy YVN (2016) Decadal land use and land cover classifications across India, 1985, 1995, 2005. ORNL DAAC, Oak Ridge, Tennessee, USA
Ryberg KR, Hodgkins GA, Dudley RW (2020) Change points in annual peak streamflows: Method comparisons and historical change points in the United States. J Hydrol 583:124307
Şen Z (2019) Partial trend identification by change-point successive average methodology (SAM). J Hydrol 571:288–299
Shuttle Radar (n.d.) Topography mission 1 arc-second global (digital object identifier (DOI) number: /https://doi.org/10.5066/F7PR7TFT). Accessed: 2020-02-01
Sinha RK, Eldho TI, Subimal G (2023) Assessing the impacts of land use/land cover and climate change on surface runoff of a humid tropical river basin in Western Ghats, India. Int J River Basin Manag 21(2):141–152
Sivapalan M, Savenije HH, Blöschl G (2012) Socio-hydrology: a new science of people and water. Hydrol Process 26(8):1270–1276
Sneyers R (1990) On the statistical analysis of series of observations (No. 551.501. 3 SNE)
Srinivasan R, Arnold JG, Jones CA (1998) Hydrologic modelling of the United States with the soil and water assessment tool. Int J Water Resour Dev 14(3):315–325
Srivastava A, Maity R (2023) Unveiling an Environmental Drought Index and its applicability in the perspective of drought recognition amidst climate change. J Hydrol 627:130462

Suman M, Maity R (2021) Assessment of basin-wise future agricultural drought status across India under changing climate. J Water Climate Change 12(6):2400–2421
Sun C, Zhou X (2020) Characterizing hydrological drought and water scarcity changes in the future: a case study in the Jinghe River Basin of China. Water 12(6):1605
Swain SS, Mishra A, Sahoo B, Chatterjee C (2020) Water scarcity-risk assessment in data-scarce river basins under decadal climate change using a hydrological modelling approach. J Hydrol 590:125260
Swain SS, Mishra A, Chatterjee C, Sahoo B (2021) Climate-changed versus land-use altered streamflow: A relative contribution assessment using three complementary approaches at a decadal time-spell. J Hydrol 596:126064
Swain SS, Kumar SB, Mishra A, Chatterjee C (2023) Sensitive or resilient catchment?: A Budyko-based modeling approach for climate change and anthropogenic stress under historical to CMIP6 future scenarios. J Hydrol 622:129651
Swain SS, Mishra A, Chatterjee C (2024) Time-varying evaluation of compound drought and hot extremes in machine learning-predicted ensemble CMIP5 future climate: a multivariate multi-index approach. J Hydrol Eng 29(2):04024001
Tan ML, Gassman PW, Yang X, Haywood J (2020) A review of SWAT applications, performance and future needs for simulation of hydro-climatic extremes. Adv Water Resour 143:103662
Tankpa V, Wang L, Awotwi A, Singh L, Thapa S, Atanga RA, Guo X (2021) Modeling the effects of historical and future land use/land cover change dynamics on the hydrological response of Ashi watershed, Northeastern China. Environ Dev Sustain 23:7883–7912
Taylor R (2009) Rethinking water scarcity: the role of storage. EOS Trans Am Geophys Union 90(28):237–238
UN World Water Development Report (2021) UN-Water. Retrieved February 5, 2024, from https://www.unwater.org/publications/un-world-water-development-report-2021
Uniyal B, Kosatica E, Koellner T (2023) Spatial and temporal variability of climate change impacts on ecosystem services in small agricultural catchments using the Soil and Water Assessment Tool (SWAT). Sci Total Environ 875:162520
Van Griensven A, Meixner T (2007) A global and efficient multi-objective auto-calibration and uncertainty estimation method for water quality catchment models. J Hydroinf 9(4):277–291
Veldkamp TIE, Wada Y, Aerts JCJH, Döll P, Gosling SN, Liu J, Masaki Y, Oki T, Ostberg S, Pokhrel Y, Satoh Y, Kim H, Ward PJ (2017) Water scarcity hotspots travel downstream due to human interventions in the 20th and 21st century. Nat Commun 8(1):15697
Visakh S, Raju PV, Kulkarni SS, Diwakar PG (2019) Inter-comparison of water balance components of river basins draining into selected delta districts of Eastern India. Sci Total Environ 654:1258–1269
Wada Y, van Beek LPH, Viviroli D, Dürr HH, Weingartner R, Bierkens MFP (2011) Global monthly water stress: 2. Water demand and severity of water stress. Water Resour Res, 47(7)
Wagener T, Sivapalan M, Troch PA, McGlynn BL, Harman CJ, Gupta HV, Kumar P, Rao PSC, Basu NB, Wilson JS (2010) The future of hydrology: an evolving science for a changing world. Water Resour Res, 46(5)
Wang Q, Xu Y, Wang Y, Zhang Y, Xiang J, Xu Y, Wang J (2020) Individual and combined impacts of future land-use and climate conditions on extreme hydrological events in a representative basin of the Yangtze River Delta China. Atmos Res 236:104805
Wang X, Erdman C, Emerson JW (2018) Bayesian analysis of change point problems
World Economic Forum (2014) WEF Global Risks
Wu C, Liu W, Deng H (2023) Urbanization and the emerging water crisis: identifying water scarcity and environmental risk with multiple applications in urban agglomerations in Western China. Sustainability 15(17):17
Wu J, An P, Zhao C, Wei Z, Lan T, Li X, Wang G (2024) Effects of multi-year droughts on the precipitation-runoff relationship: an integrated analysis of meteorological, hydrological, and compound droughts. J Hydrol, 131064

Xie P, Gu H, Sang YF, Wu Z, Singh VP (2019) Comparison of different methods for detecting change points in hydroclimatic time series. J Hydrol 577:123973

Xu Z, Han Y, Tam CY, Yang ZL, Fu C (2021) Bias-corrected CMIP6 global dataset for dynamical downscaling of the historical and future climate (1979–2100). Sci Data 8(1):293

Yang Y, Tian F (2009) Abrupt change of runoff and its major driving factors in Haihe River Catchment China. J Hydrol 374(3–4):373–383

Zhang M, Liu N, Harper R, Li Q, Liu K, Wei X, Liu S (2017) A global review on hydrological responses to forest change across multiple spatial scales: Importance of scale, climate, forest type and hydrological regime. J Hydrol 546:44–59

Zhao J, Huang Q, Chang J, Liu D, Huang S, Shi X (2015) Analysis of temporal and spatial trends of hydro-climatic variables in the Wei River Basin. Environ Res 139:55–64

Zhao J, Zhang N, Liu Z, Zhang Q, Shang C (2024) SWAT model applications: from hydrological processes to ecosystem services. Sci Total Environ, 172605

Zhou C, van Nooijen R, Kolechkina A, Hrachowitz M (2019) Comparative analysis of nonparametric change-point detectors commonly used in hydrology. Hydrol Sci J 64(14):1690–1710

Zhou J, Deitch MJ, Grunwald S, Screaton E (2023) Do the Mann–Kendall test and Theil-Sen slope fail to inform trend significance and magnitude in hydrology? Hydrol Sci J 68(9):1241–1249